Femtosecond laser inscription of depressed cladding single-mode mid-infrared waveguides in sapphire

JEAN-PHILIPPE BÉRUBÉ, JEROME LAPOINTE, ALBERT DUPONT, MARTIN BERNIER, AND RÉAL VALLÉE

Centre d'Optique Photonique et Laser (COPL)—Université Laval, 2375 de la Terrasse, Québec G1V 0A6, Canada

Accepted for publication in *Optics Letters*, November 2018

Mid-infrared optical waveguides were inscribed in sapphire with femtosecond pulses at 515 nm. We show that such pulses induce a smooth negative refractive index change allowing for the inscription of a depressed cladding waveguide by closely overlapping the corresponding type I modification traces. The resulting structure consists of a highly symmetrical, uniform, and homogeneous waveguide. The size and numerical aperture of the waveguides were tailored to achieve efficient transmission in the mid-infrared. Single mode operation at a wavelength of 2850 nm and propagation loss of <0.37 dB⁄cm are reported for a 33 mm long depressed cladding waveguide. Thermal annealing was performed, and the refractive index contrast was still preserved to 50% (i.e., $\Delta n \sim 2.5 \times 10^{-3}$) up to 1400°C.

Since its first demonstration by Davis *et al*. in 1996 [1], femtosecond laser direct inscription has evolved into an established technology and found a wide range of scientific and industrial applications. The technique has been used to develop novel photonic components such as quantum photonic circuits [2], lab-on-a-fiber [3], and on-surface refractometric sensors for liquids [4]. Lately there has been a strong incentive for the fabrication of photoinscribed devices that operate in the near and mid-infrared (IR) wavelength ranges. The mid-IR range (3–10 μm), also called the molecular fingerprint region, is of particular interest because of the presence of strong absorption from basic molecular bonds such as O—H, C—H, and C—O. As such, tremendous efforts were deployed to find optical materials that could act as adequate hosts for mid-IR photoinscribed devices. For that purpose, the two prerequisites are high transmission at the wavelength of operation and sufficient photosensitivity. Up to now, very few materials have proven to possess both. Optical waveguides that operate in the mid-IR were successfully inscribed in amorphous materials such as chalcogenide [5,6], fluoride [7], and germanate [8] glasses among others. In most cases however, one of the two requirements is partly or simply not met. An important challenge arises from the presence of hydroxyl ion impurities in glass that significantly affect the optical transmission near the water absorption bands, thus preventing or limiting a large number of sensing applications.

As such, optical crystals are a viable alternative since they generally present excellent transmission in the mid-IR and contain only traces of hydroxyl ions and other impurities [9]. However, femtosecond laser direct inscription in crystals is a more complex process than in amorphous materials. Indeed, a photoinduced increase of the refractive index through structural densification of the crystal lattice is essentially impractical. Consequently, stress-induced waveguides formed in crystals are based on damage tracks [10] (i.e., so-called type III modifications [11]) induced using high energy pulses. Photonic devices were nevertheless inscribed in this manner in a wide range of crystals [12–14] with most of the efforts focused on Nd:YAG [15] and $LiNbO_3$ [16] for waveguide lasers and nonlinear optics applications. In the mid-IR, the fabrication of waveguides in ZnSe, $LiNBO_3$, and BGO was demonstrated with propagation losses ranging between 1.5 and 4dB$\cdot$ cm^{-1} [17–19].

Sapphire is one of the hardest and most resistant optical materials and possesses an extended transmission in the mid-IR up to 5 μm. Moreover, the excellent heat conductivity and high melting temperature of sapphire makes it ideal for sensing in harsh environments [20]. Up to now, very few studies were conveyed on the photoinscription of waveguides in sapphire. Notable exceptions are reported on the fabrication of waveguides [21], waveguide lasers [22,23], and *Y* -junction splitters [24] in Ti:sapphire based on the formation of damage tracks.

In this Letter, we report the first inscription of type I related waveguides in sapphire, especially designed for the mid-IR. Specifically, the fabrication of circular, highly uniform, and single mode depressed cladding waveguides (DCW) operating at 2850 nm is demonstrated.

Waveguides were inscribed using a high-power Yb:YAG femtosecond laser (IMPULSE, Clark-MXR). The laser delivers both fundamental and frequency-doubled pulses centered at 515 nm at a repetition rate of 3.15 MHz. The pulse duration was measured to be 275 fs at the output of the laser. Pulses were focused using a 100×, 0.8 NA (Nikon, LWD) microscope objective at 180 μm below the surface of a 33 mm × 12 mm × 1mm bulk sapphire sample (Meller Optics). The sample was moved transversely with respect to the beam propagation direction using a motorized three-axis stage (Aerotech, ANT130 and PlanarDL-200XY). The sapphire crystal sample was oriented with the C-plane (0001) perpendicular to the writing beam.

It has been shown in a previous report by Elsmann *et al*. [25] that using visible pulses eases the inscription process of fiber Bragg gratings (FBGs) in sapphire fibers. As such, frequency-doubled ($\lambda = 515$ nm) low energy pulses were used to form smooth type I modifications in sapphire. It was shown that irradiation at the fundamental wavelength of the laser in otherwise similar irradiation conditions resulted in the formation of either weak and irregular type I modifications or damage tracks akin to type III modifications. Images of modification traces inscribed using both 1030 and 515 nm pulses with increasing energy are presented in Fig. 1.

From Fig. 1, it appears to be impractical to form type I modifications using near-IR pulses, with most of the tested writing conditions leading to irregular tracks with signs of damage. At this point, further analysis would be necessary to get a better insight on the inscription process involving near-IR pulses in sapphire. Nevertheless, it is observed that using 515 nm pulses greatly facilitates the inscription of smooth negative refractive index changes in sapphire.

In order to get a better assessment of the photoinduced refractive index change in the actual range of irradiation conditions that yield type I modifications, traces were inscribed with scan speed varying between 0.05 and 100 mm $\cdot$ s^{-1} using four different pulse energies (40, 50, 60, and 70 nJ). Afterward, the refractive index profile of the traces was measured using quantitative phase microscopy (QPM) (Phasics Ltd., SIDBio4) [26]. The peak of the negative index change ranged between -1×10^{-3} and -5.3×10^{-3} over the range of irradiation conditions.

To fabricate the depressed cladding waveguides, the pulse energy and the translation speed were limited to 50 nJ and 2.4mm$\cdot$ s^{-1} to prevent the formation of cracks that tend to occur when overlapping a large number of photoinduced tracks. Microscope images of the cross section along with a longitudinal view of a track written under such conditions are shown in Figs. 2(a) and 2(b). The corresponding refractive index profile is shown in Fig. 2(c), yielding a maximum negative index change of -3.4×10^{-3}.

Next, circular depressed cladding structures were inscribed by scanning the sample across the laser beam multiple times, positioning the multiple tracks along a ring-shaped pattern. This inscription method allows precise adjustment of the optical characteristics of the photoinduced waveguides. As such, the inner ($r = 8.5$ μm) and outer radii ($r = 26.5$ μm) of the DCW were chosen to achieve both efficient coupling with a single mode mid-IR zirconium fluoride fiber from Le Verre Fluoré (15/250, 0.12 NA, mode field diameter of 19 μmat $\lambda = 2850$ nm) and strong confinement in the waveguide core.

To ensure a smooth and homogenous refractive index change, the separation between the tracks that compose the cladding has to be of about 0.4 μm or less [27]. In our experiment, 705 individual tracks of 1.6×4.8 μm [see Fig. 2(a)] were therefore overlapped to a maximum separation of 0.3 μm near the DCW inner radius and increased to 1 μm near its edge as a compromise between overlap and processing time. Moreover, the spacing was varied along both transverse directions to compensate for the elliptical shape of the individual tracks and enhance the uniformity and symmetry of the index modification over the cross section.

Phase images of a DCW were obtained and an Abel transform was applied in order to retrieve the radial index profile following a procedure similar to the one detailed in [20]. An image of the cross section along with the radial refractive index profile of a DCW inscribed in sapphire are depicted in Fig. 3.

It is shown that the photoinduced refractive index change (with respect to the pristine material baseline) is kept relatively constant over the cladding, reaching a minimum of -3.8×10^{-3} close to the inner radius of the cladding and increasing slightly to -3×10^{-3} at the outer edge. The index contrast variation along the waveguide longitudinal axis was also verified and is smaller than the 2% error inherent to the QPM measurement [26]. Even though only the cladding region is irradiated with focused pulses, an increase of the relative index change of $\sim 1 \times 10$ qpm^{-3} is observed both in the core region and right outside the depressed cladding region. This effective index increase in nonirradiated regions is related to the stress induced by the expansion of the irradiated material [10]. Thus, the benefit of the strongly overlapped cladding structure is two-fold. It allows precise control of the size and numerical aperture of the waveguide and of the stress-induced positive index change in the center, further enhancing the confinement of light. The refractive index contrast based on smooth type I modifications also allows for waveguides with bend radius similar to core waveguides [28]. Hence, for waveguides with an effective index contrast close to 5×10^{-3}, such as the one shown in Fig. 3, bend radii as short as 10 mm can be accommodated without additional loss.

Next, light emitted by an erbium-doped fluoride glass fiber laser ($\lambda = 2850$ nm)[29] was butt-coupled to the waveguide. The near-field intensity profile at the output was imaged unto a thermal imaging camera (Telops TS-IR MW) using a $f = 50$ mm ZnSe lens. Results are shown in Fig. 4.

It is seen that 2850 nm light is strongly confined in the DCW. The mode was measured to be 19.2 and 18.4±0.3 μm evaluated at e^{-2} of the maximum intensity along both transverse directions. This is in agreement with the expected mode field diameter of 18.8 μm calculated considering the actual refractive index profile of the DCW [as shown in Fig. 3(b)]. Note that no stray or scattered light is observed outside the core region.

Afterward, the outcoupling lens was removed and replaced by another piece of single mode fluoride fiber which was butt-coupled to the output end face of the waveguide. Light was directed to a power meter (Gentec XLP12), and the optical transmission of the 33.25 mm long DCW was monitored. A reference was taken prior to and after the measurement by removing the sample and coupling light directly between the two single mode fibers. A total insertion loss of 1.9 dB was inferred from this measurement. The insertion losses include reflection at the air–crystal interfaces, mode mismatch with the input fiber, fiber to waveguide misalignment, bulk attenuation, and propagation losses. Taking into account negligible bulk attenuation and fiber to waveguide misalignment, 0.62 dB for the Fresnel reflections ($n = 1.715$ at $\lambda = 2850$ nm) and a calculated mode mismatch between the DCW and the input and output fibers of 0.05 dB, losses of 1.1 dB remain. As such, an upper bound of 0.37 dB/cm for the propagation losses is obtained.

Then, the transmission of the waveguide was evaluated while varying the orientation of the input linear polarization using free space optics at $\lambda = 800$ nm. It was revealed that the waveguide is polarization insensitive as no significant variation of the transmission was recorded. This was expected given the remarkable symmetry exhibited by the DCW and represents a considerable upgrade over stress-induced waveguides, which typically suffer from polarization-selective transmission [21].

Next, six similar DCW were inscribed in a separate 1 mm thick, 10 mm × 14 mm sapphire sample in order to perform thermal annealing. The waveguides were inscribed with increasing pulse energies and a fixed translation of 2mm· s^{-1}. Prior to the annealing process, the refractive index profiles of the six waveguides were monitored. Then the sample was placed in a thermal furnace (Mellen Microtherm MS Box 1550), heated up slowly over 7 h to the annealing temperature, maintained for 1 h, and cooled down following a 7 h linearly decreasing ramp. The sample was successively exposed to temperatures of 750, 1000, and 1400°C, and the refractive index profiles of the waveguides were measured between each cycle. The radial refractive index profiles of a DCW and the peak negative index change of the DCW inscribed with increasing pulse energy for each annealing temperature are depicted in Fig. 5.

Figure 5 shows that DCWs inscribed in sapphire are unaffected by temperature at least up to 1000°C. A peak index change of -2.5×10^{-3} was maintained after heating up to 1400°C for a DCW that exhibited -4.75×10^{-3} prior to the annealing process. Also, no alteration of the size and morphology of the DCW was observed. The index change begins to decrease at a temperature between 1000 and 1400°C, which corresponds respectively to 50% and 70% of the melting temperature (T_m = 2040°C) of sapphire. Our results are in agreement with previous studies of the thermal stability of FBGs inscribed in single-crystal sapphire fibers [25,30]. Also, the transmission of the waveguides at λ = 2850 nm was evaluated after the annealing process, and no significant change was observed. The mode field increased from 19.2 to 23.7± 0.3 μm, which was expected given the weaker index change.

In conclusion, we have demonstrated for the first time the inscription of low-loss mid-IR waveguides in sapphire. The formation of smooth type I modifications using visible femtosecond pulses at λ = 515 nm is reported. Using this inscription method, depressed cladding waveguides were formed by overlapping a large number of tracks. The resulting cladding based on a highly symmetrical and homogeneous index change proved advantageous over the structures based solely on the stress induced by damage lines traditionally inscribed in crystals. Precise control over both the size and numerical aperture of the DCW is achieved, which allows for the fabrication of single mode waveguides at any given target wavelength. As such, the DCW optical characteristics were carefully adjusted for single mode operation at a wavelength of 2850 nm. Efficient coupling with single mode mid-IR fibers and propagation losses of <0.37 dB⁄cm are reported at this wavelength. Lastly, the DCWs were subjected to successive heating cycles up to a temperature of 1400°C. The waveguides were preserved without alteration of shape, size, and magnitude of the index change up to 1000°C. Our results pave the way for the fabrication of low loss mid-IR devices in crystals, thus opening novel avenues for the development of a wide range of applications, namely fiber sensing in harsh environments.

Funding

Natural Sciences and Engineering Research Council of Canada (NSERC) (IRCPJ469414-13); Canada Foundation for Innovation (CFI) (37422).

Acknowledgment

The authors wish to thank Yannick Ledemi and Vincent Fortin for meaningful discussions and assistance.

References

[1] K. Davis, K. Miura, N. Sugimoto, and K. Hirao, Opt. Lett. 21, 1729 (1996).

[2] A. Crespi, R. Osellame, R. Ramponi, D. Brod, E. Galvao, N. Spagnolo, C. Vitelli, E. Maiorino, P. Mataloni, and F. Sciarrino, Nat. Photonics 7, 545 (2013).

[3] M. Haque, K. K. Lee, S. Ho, L. A. Fernandes, and P. Herman, Lab Chip 14, 3817 (2014).

[4] J. Lapointe, F. Parent, E. Soares de Lima Filho, S. Loranger, and R. Kashyap, Opt. Lett. 40, 5654 (2015).

[5] J. Bérubé, S. Messaddeq, M. Bernier, I. Skripachev, R. Vallée, and Y. Messaddeq, Opt. Express 22, 26103 (2014).

[6] A. Ródenas, G. Martin, B. Arezki, N. Psaila, G. Jose, A. Jha, L. Labadie, P. Kern, A. Kar, and R. Thomson, Opt. Lett. 37, 392 (2012).

[7] S. Gross, N. Jovanovic, A. Sharp, M. Ireland, J. Lawrence, and M. J. Withford, Opt. Express 23, 7946 (2015).

[8] J. Bérubé, A. Le Camus, S. Messaddeq, Y. Petit, Y. Messaddeq, L. Canioni, and R. Vallée, Opt. Mater. Express 7, 3124 (2017).

[9] J. Harrington, D. Gregory, and W. J. Otto, Appl. Opt. 15, 1953 (1976).

[10] F. Chen and J. V. de Aldana, Laser Photon. Rev. 8, 251 (2014).

[11] B. Poumellec, M. Lancry, A. Chahid-Erraji, and P. Kazansky, Opt. Mater. Express 1, 766 (2011).

[12] T. Calmano and S. Muller, IEEE J. Sel. Top. Quantum Electron. 21, 401 (2015).

[13] A. Courvoisier, M. Booth, and P. Salter, Appl. Phys. Lett. 109, 031109 (2016).

[14] W. Nie, Y. Jia, J. V. de Aldana, and F. Chen, Sci. Rep. 6, 22310 (2016).

[15] G. Salamu, F. Jipa, M. Zamfirescu, and N. Pavel, Opt. Express 22, 5177 (2014).

[16] J. Lv, Y. Cheng, W. Yuan, X. Hao, and F. Chen, Opt. Mater. Express 5, 1274 (2015).
[17] J. MacDonald, S. Beecher, P. Berry, K. Schepler, and A. Kar, Appl. Phys. Lett. 102, 161110 (2013).
[18] H.-D. Nguyen, A. Rodenas, J. V. de Aldana, G. Martin, J. Martinez, M. Aguilo, M. C. Pujol, and F. Diaz, Opt. Express 25, 3722 (2017).
[19] R. He, I. Hernandez-Palmero, C. Romero, J. V. de Aldana, and F. Chen, Opt. Express 22, 31293 (2014).
[20] M. Busch, W. Ecke, I. Latka, D. Fischer, R. Willsch, and H. Bartlet, Meas. Sci. Technol. 20, 115301 (2009).
[21] J. Bai, G. Cheng, X. Long, Y. Wang, W. Zhao, G. Chen, R. Stoian, and R. Hui, Opt. Express 20, 15035 (2012).
[22] S. Gross, M. Withford, and A. Fuerbach, Proc. SPIE 7589, 75890U (2010).
[23] C. Grivas, C. Corbari, G. Brambilla, and P. Lagoudakis, Opt. Lett. 37, 4630 (2012).
[24] Y. Ren, L. Zhang, H. Xing, C. Romero, J. V. de Aldana, and F. Chen, Opt. Laser Technol. 103, 82 (2018).
[25] T. Elsmann, T. Habisreuther, A. Graf, M. Rothhardt, and H. Bartelt, Opt. Express 21, 4591 (2013).
[26] E. Bélanger, J. Bérubé, B. De Dorlodot, P. Marquet, and R. Vallée, Opt. Express 26, 17498 (2018).
[27] G. Douglass, F. Dreisow, S. Gross, S. Nolte, and M. Withford, Opt. Express 23, 21392 (2015).
[28] N. Charles, N. Jovanovic, S. Gross, P. Stewart, B. Norris, J. O'Byrne, J. Lawrence, M. Withford, and P. Tuthill, Appl. Opt. 51, 6489 (2012).
[29] V. Fortin, M. Bernier, S. Bah, and R. Vallée, Opt. Lett. 40, 2882 (2015).
[30] D. Grobnic and S. J. Mihailov, IEEE Photon. Technol. Lett. 16, 2505 (2004).

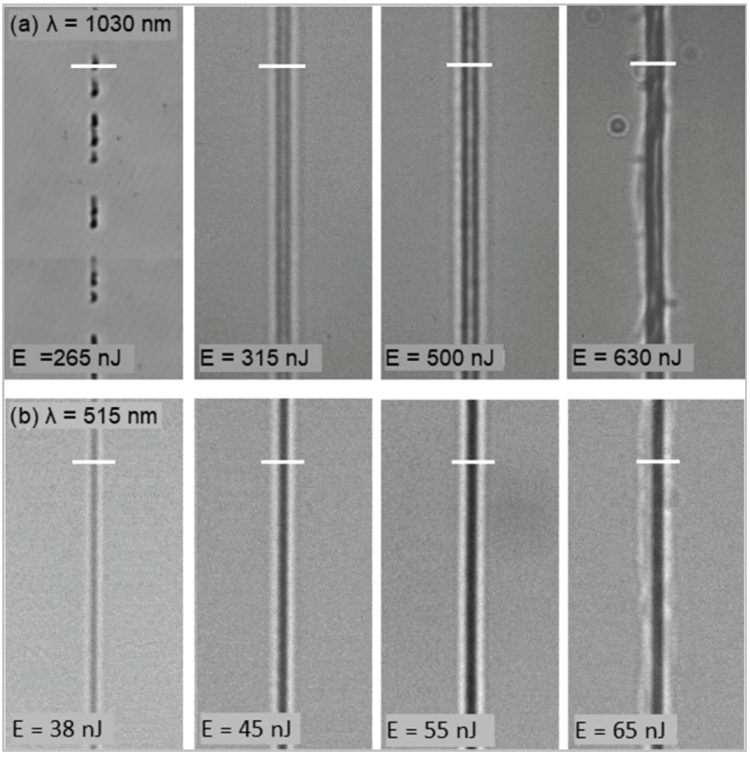

Fig. 1. Photoinduced modification tracks inscribed using (a) 1030 nm and (b) 515 nm pulses with increasing pulse energy. Translation speed: $v = 1$ mm · s^{-1}. The white scale bars equal 5 μm.

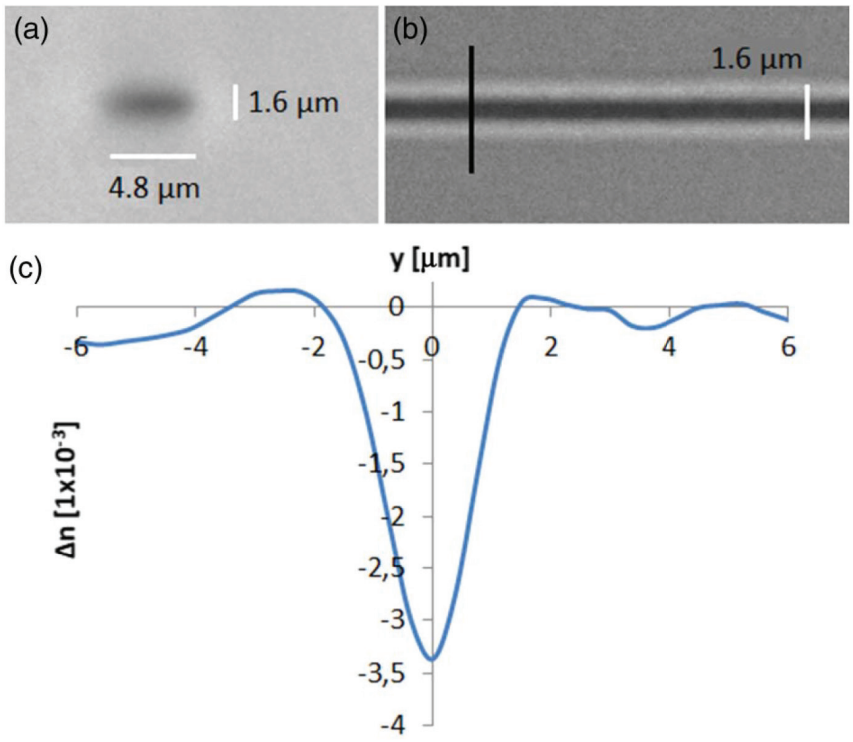

Fig. 2. (a) Cross section and (b) longitudinal images of tracks inscribed in sapphire. E = 50 nJ, v = 2.4mm· s^{-1}. (c) Refractive index profile measured along the white line.

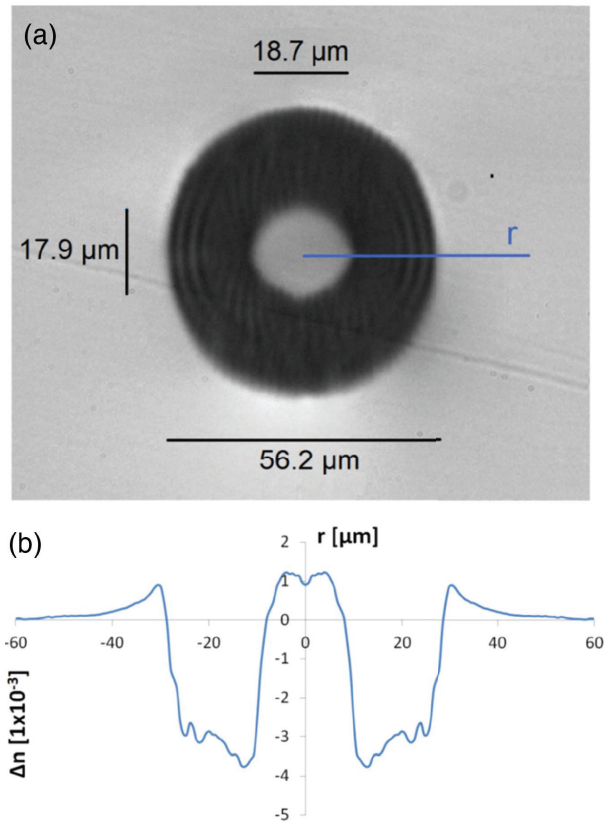

Fig. 3. (a) Image of the cross section and (b) radial refractive index profile of a DCW inscribed in sapphire. The profile is computed along the solid blue line, and data are plotted symmetrically on both sides of the central axis.

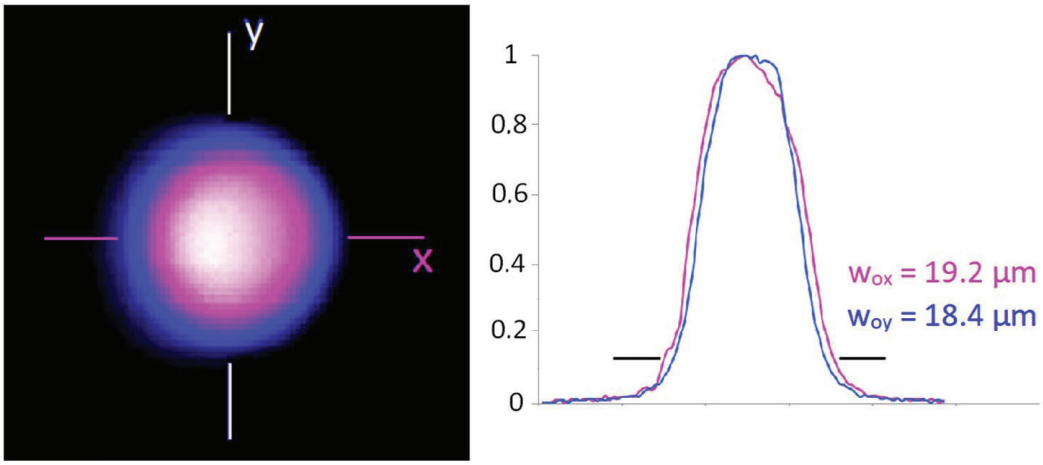

Fig. 4. Near-field intensity profile measured at the output of the DCW waveguide of transmitted light at a wavelength of 2850 nm.

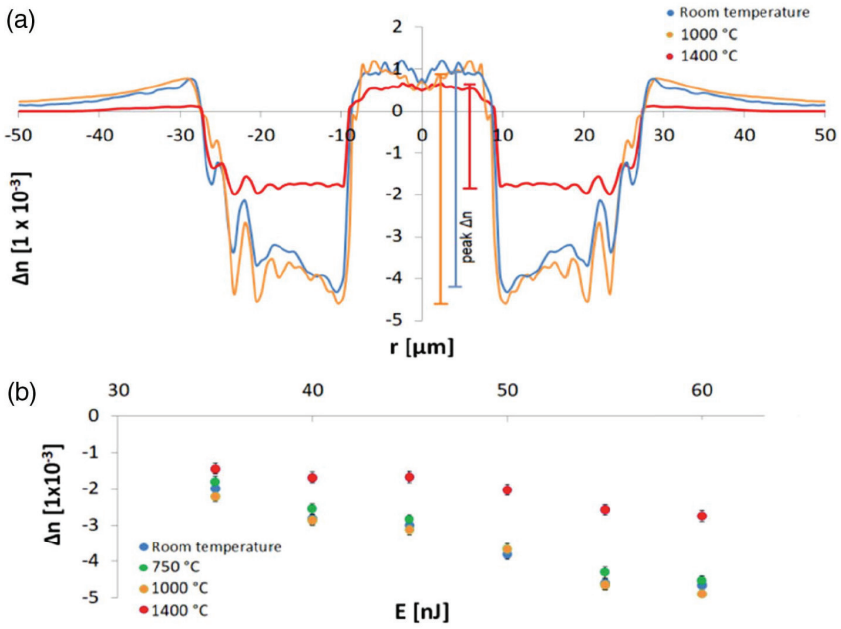

Fig. 5. (a) Radial refractive index profiles measured after successive annealing cycles. (b) Peak index change of DCW inscribed with increasing pulse energy for different annealing temperatures.